HHS Public Access

Author manuscript

J Biomed Mater Res A. Author manuscript; available in PMC 2016 June 23.

Published in final edited form as:

J Biomed Mater Res A. 2014 May ; 102(5): 1486–1499. doi:10.1002/jbm.a.34799.

Host Response to Microgel Coatings on Neural Electrodes Implanted in the Brain

Stacie M. Gutowski[1,2], **Kellie L. Templeman**[1,4], **Antoinette B. South**[3], **Jeffrey C. Gaulding**[3], **James T. Shoemaker**[1,2], **Michelle C. LaPlaca**[1,2], **Ravi V. Bellamkonda**[1,2], **L. Andrew Lyon**[1,3], and **Andrés J. García**[1,4,*]

[1]Petit Institute for Bioengineering and Bioscience, Georgia Institute of Technology, Atlanta, Georgia 30332-0363

[2]Coulter Department of Biomedical Engineering, Georgia Institute of Technology, Atlanta, Georgia 30332-0363

[3]School of Chemistry and Biochemistry, Georgia Institute of Technology, Atlanta, Georgia 30332-0400

[4]Woodruff School of Mechanical Engineering, Georgia Institute of Technology, Atlanta, Georgia 30332-0363

Abstract

The performance of neural electrodes implanted in the brain is often limited by host response in the surrounding brain tissue, including astrocytic scar formation, neuronal cell death, and inflammation around the implant. We applied conformal microgel coatings to silicon neural electrodes and examined host responses to microgel-coated and uncoated electrodes following implantation in the rat brain. *In vitro* analyses demonstrated significantly reduced astrocyte and microglia adhesion to microgel-coated electrodes compared to uncoated controls. Microgel-coated and uncoated electrodes were implanted in the rat brain cortex and the extent of activated microglia and astrocytes as well as neuron density around the implant were evaluated at 1, 4, and 24 weeks post-implantation. Microgel coatings reduced astrocytic recruitment around the implant at later time points. However, microglial response indicated persistence of inflammation in the area around the electrode. Neuronal density around the implanted electrodes was also lower for both implant groups compared to the uninjured control. These results demonstrate that microgel coatings do not significantly improve host responses to implanted neural electrodes and underscore the need for further improvements in implantable materials.

Keywords

electrode; cell adhesion; microgel; polymer coating; inflammation; implantation

[*]Corresponding author: Prof. A. J. García, Woodruff School of Mechanical Engineering, Petit Institute for Bioengineering and Bioscience, Georgia Institute of Technology Atlanta, GA 30332-0363, USA, andres.garcia@me.gatech.edu.

Introduction

Neuroprosthetic devices have the potential to restore functionality to patients affected by injuries and pathologies including sensory loss, neurological disorders, spinal cord injuries, and limb amputation[1–4]. Devices that provide an interface between brain and machine require the use of neural electrodes that can receive and/or transmit electrical signals from neurons in the brain[1–4]. A significant problem with current electrode technology is recording failure of electrodes over time. Devices implanted in the body provoke an inflammatory response from the surrounding tissue, which can lead to scar formation and failure of the implant over time [5]. Electrode failure involves host responses in the tissue surrounding the electrode including increased glial scar formation and a decrease in neurons due to cell death around the electrode[6–8]. Additionally, activation of microglia around implanted electrodes supports a role for inflammation in the tissue response around the implant[7]. Maintenance of recording ability varies from days to many months, however the time frame of electrode functionality is highly variable even between electrodes in the same array and many electrodes can fail within a matter of weeks after implantation[1]. In order to improve long-term electrode functionality, it is important to introduce a device that will elicit minimal reaction from the surrounding tissue[9]. By incorporating materials that reduce astrocytic and microglial cell adhesion, it may be possible to reduce scar formation around implanted materials.

To improve the tissue response to implanted neural electrodes, several groups have applied coatings to the electrode surface as a potential solution. Coatings with an incorporated peptide sequence derived from laminin promote neuronal cell adhesion and migration[10–12], as well as coatings containing brain-derived neurotrophic factor[13]. Whereas these coatings may increase neuronal cell numbers around the electrode, they may also promote adhesion of other cell types including astrocytes, one of the main cell types involved in scar formation. Recent work by Winslow et al[14] has demonstrated a lack of improved tissue response with cell adhesion resistant coatings, indicating the possible role of persistent inflammation in the long-term tissue response that results in electrode failure. Other studies have investigated releasing anti-inflammatory agents including α-melanocyte stimulating hormone[15] and dexamethasone[16–18] to attenuate the inflammatory response of the surrounding tissue. While this research has introduced many improvements to the field, there has been limited success in improving long-term cellular response as a whole for time points longer than several weeks, and much work still remains to mediate the problems involved with chronically implanted electrode failure.

In the present study, we engineered a conformal microgel coating to reduce cell adhesion on neural electrodes. This coating consists of multi-layers of cross-linked microgel particles composed mainly of poly(*N*-isopropylacrylamide) (pNIPAm), which is cross-linked with poly(ethylene glycol diacrylate) (PEG-DA). Under physiological conditions, the PEG chains decorate the surface of the pNIPAm microgels, serving as a non-fouling coating that has been shown to reduce protein adsorption and cell adhesion, as well as reduce inflammation *in vivo*[19–21]. The microgel coating is tethered to the surface of silicon electrodes which are manufactured for neural recording applications[22]. We evaluated *in vitro* cell adhesion and host responses to microgel-coated and uncoated electrodes implanted in the rat brain.

Methods

Microgel coating of electrodes

The electrode modifier used for this study is a thermo-responsive, microstructured, hydrogel coating. This coating consists of multilayers of particles of copolymer poly(*N*-isopropylacrylamide) (pNIPAM) and acrylic acid (AAc) (pNIPAm-*co*-AAc) cross-linked with poly(ethylene glycol) (PEG) chains. Particle size and composition were previously verified by dynamic light scattering and NMR, respectively[21]. Microgel coatings were applied to the surface of electrodes made of silicon and iridium. Electrodes were purchased from NeuroNexus Technologies (CM16 A4x4-4mm-200-200-1250). Each electrode is 4 mm long with 4 active sites on each of 4 prongs, and each active site has an area of 1,250 μm^2. Non-recording electrodes were used as they are significantly less expensive than functional electrodes.

Preliminary studies indicated variable application of coatings due to organic contaminants on the as-received electrode surface. Several cleaning protocols were evaluated by surface analyses and reproducible application of coating. An optimal cleaning procedure consisting of serial 5-minute incubations in trichloroethylene (Mallinckrodt/JT Baker), acetone (Sigma-Aldrich), and methanol (Sigma-Aldrich) was used. Electrodes were then rinsed with absolute ethanol (Sigma-Aldrich). Following the cleaning procedure, electrodes were incubated in absolute ethanol for one hour. The surface was functionalized using a silane-based adhesion layer. Silicon has a natural oxide layer approximately 1 nm thick, and this layer was utilized for silanization of the surface. The electrodes were incubated for two hours with 1% 3-aminopropyl trimethoxysilane (APTMS, TCI America) in absolute ethanol. The substrate was then rinsed with ethanol and equilibrated in PBS. Anionic microgels were then added and Coulombic attraction between the cationic amine-modified silicon surface and anionic microgels resulted in the formation of a microgel monolayer. To further stabilize the initial layer, chemicals for carbodiimide coupling were used consisting of N-(3-dimethylaminopropyl)-N′-ethylcarbodiimide hydrochloride (EDC), N-hydroxysuccinimide (NHS), and hydroxylamine hydrochloride. Standard EDC/NHS coupling was used[23] to covalently attach the microgels to the silicon surface. Complete coverage of the surface with microgels was achieved by depositing four layers of microgels to coat the electrode surface. A cationic glue, polydiallyl dimethyl ammonium chloride (PDADMAC), was used between layers to promote multi-layer formation. Presence of the microgel coating was verified with atomic force microscopy (AFM) and X-ray photoelectron spectroscopy (XPS) (Fig. 1). Upon completion of coating, or after cleaning for uncoated samples, electrodes were placed in PBS until experimentation, where further cleaning/sterilization was performed (as described below).

In Vitro Cell Adhesion

Either uncoated or microgel-coated electrodes were adhered to a glass coverslip using UV-cure adhesive (NOA 68, Norland Adhesives). A single coverslip with attached electrode sample was placed in an individual well of a 12-well plate (n=3, each group). The samples were washed twice with 70% ethanol followed by three washes with sterile PBS. Mixed astrocyte and microglial cells were added to each well at a density of 50,000 cells/cm^2

(~190,000 cells/well). The samples were cultured in DMEM/F12 (Invitrogen) + 10% FBS (Invitrogen) at 37 ºC and 5% CO_2 for 24 hours. Samples were stained with LIVE/DEAD stain (Invitrogen) and imaged with a 20X Apo Nikon objective (0.75 NA). Cell spread area on the electrode surface was measured using ImageJ software (NIH).

Electrode Implantation

NIH guidelines for the care and use of laboratory animals (NIH Publication #85-23 Rev. 1985) were observed. All surgical procedures were approved by the Institutional Animal Care and Use Committee at the Georgia Institute of Technology. The electrode implantation procedure is adapted from the protocol by McConnell et al.[24] Electrodes (uncoated, microgel-coated) were rinsed with ethanol for 24 hours then washed with sterile PBS prior to implantation in the brain cortex of a rat, one per animal (n=4 animals for all groups except n=3 for uncoated at 24 weeks, similar sample sizes were used in other studies[25–27]). Male Sprague-Dawley rats (Charles River Laboratories) were anesthetized with isoflurane. The surgical site was shaved, cleaned with chlorohexaderm, and rinsed with isopropyl alcohol before mounting the animal onto a stereotactic frame. Marcaine (0.15 mL of 0.5%) was injected subcutaneously at the site of incision. A midline incision 2–3 cm long was made in the scalp and the periosteum retracted to expose the cranium. Five 1 mm-diameter pilot holes were made around the skull, four posterior to bregma, with two each on either side of the midline and one additional hole made anterior and right of bregma. A 4.7 mm stainless steel bone screw (Fine Science Tools 19010-00) was inserted into each of the pilot holes, with each screw penetrating the skull but leaving about 1–2 mm of each screw head remaining out of the skull to serve as an attachment point for the headcap. The craniotomy for electrode insertion was made anterior to and left of bregma using a 2.7 mm trephine bit (Fine Science Tools 18004-27). The electrode was held in the stereotactic frame above the 2.7 mm hole and slowly lowered into the cortex, careful to avoid any large vasculature in the surgical area. Agarose gel (1.5% w/v, SeaKem) was filled into the opening around the electrode and dental acrylic (OrthoJet, Inc.) was used to anchor the electrode assembly to the skull. The scalp incision was closed via wound clips and triple-antibiotic ointment was applied to the wound. Each animal was given an injection of 5 mL saline and allowed to recover from anesthesia before receiving a 0.03 mg/kg buprenorphine injection for pain relief. All animals were fully ambulatory post recovery.

At the designated time point (1, 4, and 24 weeks), the animal was anesthetized prior to transcardial perfusion with 200 mL 0.4% papaverine HCl in 0.9% NaCl, followed by 50 mL of 0.9% NaCl, and 200 mL of 4% paraformaldehyde in phosphate buffer. After perfusion, the skull was opened and the brain retrieved from the skull cavity. All samples were kept in 4% paraformaldehyde in phosphate buffer solution overnight then placed in 30% sucrose in PBS until the brain sank to the bottom of a 50 mL conical tube. Samples were embedded in OCT and frozen using isopentane in liquid nitrogen.

Histological Evaluation

Samples were sectioned in 16 μm-thick sections using a cryostat and stained for various cell markers as indicated in Table 1. All primary antibodies were visualized with AlexaFluor 488 secondary antibody (Invitrogen) and counterstained with DAPI for cell nuclei recognition.

Upon completion of staining, all slides were imaged using a 10X Nikon objective (0.30 NA) and SPOT Advanced software (Diagnostic Instruments, Inc.).

Data obtained from *in vivo* studies were analyzed using MATLAB software (Mathworks). A line was drawn manually along the edge of the injury caused by the electrode and the intensity values were gathered starting at the edge of the injury and moving 500 μm perpendicularly from the line (Fig. 3a)[28]. For GFAP, ED1, and OX42 staining, the average intensity was normalized to the intensity of the contralateral [background] image by utilizing point by point subtraction of the background staining (obtained from the corresponding contralateral uninjured hemisphere) from the injury image, taking into account the variation of field illumination. This method allows for subtracting the uninjured tissue staining of resident cells (GFAP and OX42), subtraction of the background (ED1), and accounting for the variation in field illumination in all samples. The normalized intensity per trajectory was plotted, yielding a curve indicating the intensity variation as a function of distance (x) from the edge of the implanted electrode (Fig. 3a, right). Each curve was fit to equation 1 and a five-parameter fit applied to each curve.

$$normalized\ intensity = intensity_1 * e^{-decay_1{}^x} + intensity_2 * e^{-decay_2{}^x + f.} \quad \text{Equation 1}$$

This equation was chosen for the curve fit because there are two intensity and decay parameters in the equation corresponding to the initial steep decay in the intensity at distances corresponding to 0–100 μm (parameters: $intensity_1$ and $decay_1$) followed by a slower rate of decay at distances >100 μm from the edge of injury (parameters: $intensity_2$ and $decay_2$). Samples from each animal were used to generate independent intensity curves for each marker (GFAP, OX42/CD11b, ED1/CD68). The intensity curves for each individual animal were then combined and analyzed to obtain an inter-animal average per group for each marker at each time point. Analysis for NeuN staining utilized a similar methodology by analyzing cell staining starting at the scar and moving 500 μm away from the injury. However, staining is analyzed by counting NeuN+ cells[28] per 100 μm bin (Fig. 3b), as the staining for NeuN is either positive or negative for neuronal nuclei, with the number of positive cells indicating the number of neuronal nuclei in the analysis area. The number of NeuN+ cells is then plotted as a percentage of the corresponding uninjured control (contralateral hemisphere) (Fig 3b, bottom). Samples from each animal were combined to obtain an inter-animal average per group for NeuN at each time point.

Statistical Analysis

Data presented are mean +/− standard error. Statistical analyses for differences in the *in vitro* cell adhesion study were performed using a two-tailed t-test in JMP Pro10 (SAS Software). Mean and standard error for parameters of curve fits from non-linear regression ($intensity_1$, $intensity_2$, $decay_1$, $decay_2$) for GFAP, OX42, and ED1 for uncoated and microgel-coated samples were obtained using the two-phase decay equation (Equation 1) in Graphpad Prism 6.0. Statistical analyses for differences between the two groups at a given time point were performed using a t-test, and analysis for differences in parameters over time were performed using ANOVA. Staining for NeuN+ cells was analyzed per 100 μm bin and

compared between uncoated samples, microgel-coated samples, and contralateral uninjured controls using ANOVA in JMP Pro10 (SAS Software). Post-hoc testing consisted of Dunnett's method to test for differences between the contralateral (uninjured control) and experimental (uncoated and microgel-coated) samples, and Tukey-Kramer HSD test was used to test for differences between uncoated and microgel-coated samples in each bin per time point. A p-value of <0.05 was considered significant.

Results

Characterization of Microgel Coatings

Microgel coatings were characterized using atomic force microscopy (AFM) and X-ray photoelectron spectroscopy (XPS) to validate morphology and chemical composition. Figure 1a shows the molecular structure of the microgels consisting of N-isopropylacrylamide (NIPAm; 70.5 mol%), acrylic acid (AAc; 26 mol%), and the crosslinker poly(ethylene glycol) diacrylate (MW=575, PEGDA-575; 3.5 mol%). AFM analysis of electrodes that were cleaned, incubated with only APTMS and PDADMAC, and microgel-coated indicated a uniform conformal coating of microgels on the surface of the microgel-coated electrode (Figure 1b). The microgel coating covered both the silicon substrate as well as the iridium wire that is used for transmission of the electrical signal. As this study only utilized non-recording electrodes for the purposes of histological evaluation, no tests were performed to observe changes in impedance at the electrode recording sites. However, because of the high water content of these films (~90%), we do not expect significant changes in the electrical impedance of the device. AFM analysis to determine wet thickness of the microgel coating was performed by introducing a scratch into the coating with a razor blade, exposing the bare substrate next to the microgel-coated area, and measuring the thickness of the coating in relation to the bare substrate. This analysis indicated microgel coating thickness of ~60 nm, which is consistent with previous studies[29]. Figure 1c indicates the change in chemical composition of the surface as analyzed by XPS. The presence of Si peaks is likely due to collapse of the microgel coating under vacuum within the penetration depth of the technique. Note the change in XPS spectra indicating increased carbon and nitrogen peaks on the microgel-coated electrodes corresponding to deposition of a coating on the electrode surface. Taken together, the AFM and XPS results demonstrate application of a uniform, conformal microgel coating on neural electrodes.

In Vitro Cell Adhesion

Uncoated and microgel-coated electrodes were seeded with mixed glial cells (astrocytes + microglia) to evaluate adhesion to these materials. Analysis of results from the *in vitro* experiment indicates the effectiveness of the microgel coating for reducing cell adhesion on the surface of electrodes as well as high viability (>99%) of plated cells. Similar cell density and cell spreading were observed on the glass coverslip beneath each sample, indicating continuity of cell seeding and spreading between samples (Figure S1). There was significantly reduced cell adhesion and cell spreading on the microgel-coated electrode surface as compared to the uncoated control (Fig. 2a). Each of these representative images shows significantly higher cell adhesion and spreading on the uncoated electrodes whereas the microgel-coated images indicate very few cells attached to the surface and reduced cell

spreading. The total cell spreading was analyzed by taking a series of images along the length of the electrode and averaging total cell spread area per electrode. Cell spread area was quantified (Fig. 2b) by determining the area of the cells present on the electrode surface using ImageJ area measurement tool. There was a significant difference in cell spread area between the samples, with approximately 60 times lower cell adhesion on microgel-coated samples compared to uncoated controls.

Host Response of Electrodes Implanted in the Brain

Microgel-coated electrodes and uncoated controls were implanted into the rat cortex. Tissue responses in the vicinity of the electrode were analyzed at three time points: 1 week, 4 weeks, and 24 weeks using immunostaining of cryosectioned samples. Image analysis was implemented to quantify levels of markers associated with neuroinflammation and neuronal cell survival (Fig. 3). Markers associated with neuroinflammation comprised GFAP (astrocytes), OX42/CD11b (resident macrophages), and ED1/CD68 (activated macrophages). Each of these markers was used to stain sections from all animals. Images from each sample were analyzed and staining intensities for each marker over a distance of 500 μm perpendicular from the edge of the electrode injury were evaluated. These intensity profiles were then fit using non-linear regression to Equation 1. In this equation, the initial set of parameters, $intensity_1$ and $decay_1$, correspond to the initial steep descent of the intensity curve and represent the host response in area closest to the electrode surface at distances ≤100 μm. The second set of parameters, $intensity_2$ and $decay_2$, correspond to the second phase of the curve with gradual descent of the intensity, indicating cell response in the area farther from the electrode at distances >100 μm.

Representative images of immunostaining for GFAP (astrocytes, Fig. 4a) show the progression of astrocytic scar formation as well as representative intensity curves (Fig. 4b, Fig. S2) at 1 week, 4 weeks, and 24 weeks. Plots of the curve fit parameters for intensity (Fig. 4c) indicate changes in the parameters over time. At 1 week, the microgel-coated samples had higher staining for $intensity_1$, $decay_1$, and $intensity_2$ parameters while $decay_2$ was lower compared to uncoated electrodes. There were also significant increases for $intensity_1$ and $decay_1$ for both uncoated and microgel-coated samples from 1 to 4 weeks, while the $decay_2$ parameter decreased for uncoated samples. At 4 weeks, staining for $intensity_1$, $decay_1$, and $decay_2$ parameters were higher for microgel-coated samples while $intensity_2$ was higher for uncoated samples. From 4 to 24 weeks $intensity_1$ and $decay_1$ decreased for microgel-coated electrodes. At 24 weeks, all parameters were higher for uncoated electrodes than microgel-coated electrodes.

OX42 staining (resident microglia, Fig. 5a) and representative intensity curves (Fig. 5b, Fig. S2) were analyzed in a similar manner to GFAP, with curve fit parameters represented in Fig. 5c. At 1 week, $intensity_1$ and $decay_2$ were higher for uncoated samples while $intensity_2$ and $decay_1$ were higher for microgel-coated samples. From 1 to 4 weeks, $decay_1$ increased for microgel-coated samples whereas $decay_2$ decreased for uncoated electrodes. At 4 weeks, all parameters were higher for microgel-coated electrodes compared to uncoated controls. From 4 to 24 weeks $decay_1$ decreased for microgel-coated samples. At 24 weeks, uncoated

samples had higher intensity$_1$ and decay$_1$ and lower intensity$_2$ parameter values than microgel-coated samples.

Results for ED1 staining (activated microglia, Fig. 6a) and representative intensity curves (Fig. 6b, Fig. S2) indicated the changes in parameters over time (Fig. 6c). At 1 week, intensity$_1$ and intensity$_2$ were higher for uncoated electrodes compared to microgel-coated electrodes. From 1 to 4 weeks, decay$_1$ and intensity$_2$ parameters decreased for uncoated electrodes while decay$_1$ increased for microgel-coated samples. At 4 weeks intensity$_1$, intensity$_2$, and decay$_2$ were all higher for uncoated samples while decay$_1$ was lower than that for microgel-coated samples. From 4 to 24 weeks, parameters for uncoated electrodes increased for intensity$_1$ and decay$_1$ while decay$_1$ decreased for microgel-coated samples. At 24 weeks, intensity$_1$, decay$_1$, and intensity$_2$ were higher and decay$_2$ was lower for uncoated electrodes compared to microgel-coated electrodes.

Data obtained from NeuN (neuronal nuclei) staining was analyzed such that each image was divided into five 100 μm bins, allowing for each NeuN+ cell to be counted and normalized to the uninjured contralateral side (Fig. 3b). Each image was plotted with the first bin starting at the edge of the implant. The number of NeuN+ cells per bin were plotted to determine changes in neuronal density for each group. Representative images of NeuN staining (Fig. 7a) indicated the presence of neuronal nuclei in each sample group, as quantified in Fig. 7b. At 1 week the uncoated and micorgel-coated samples were significantly lower than the contralateral (control) samples at 0–100 μm and 100–200 μm bins for both groups. At 4 weeks, NeuN+ staining around uncoated samples was significantly lower than microgel-coated samples at 0–100 μm, and both groups were significantly lower than the contralateral control at the same distance. Additionally, the uncoated samples were significantly lower than the contralateral control at 200–300 μm. At 24 weeks, the microgel-coated samples had significantly lower neuronal density than the contralateral control at 0–100 μm and 100–200 μm, as well as significantly lower neuronal density compared to the 4 week time point in the 400–500 μm bin.

Discussion

We have engineered a microgel coating for neural electrodes consisting of poly(NIPAm-*co*-AAc-PEG(575)-DA) particles that is applied to the surface of the electrodes using crosslinking chemistry and cationic “glue”. Previous work from our lab has shown success with the monolayer microgel coatings for reducing cell adhesion and protein adsorption[19,30], as well as significantly reducing acute and chronic inflammatory responses.[20] We have also observed moderate effects in reducing fibrous capsule formation in chronic implantation.[21] The multilayer coating used in this study performed well *in vitro* with cell adhesion experiments with mixed astrocyte and microglia cultures showing a significant reduction in the number of adherent cells and amount of cell spreading on microgel-coated electrodes compared to uncoated controls. However, the *in vivo* data obtained from chronic implantation of the electrode into the rat cortex indicated only modest improvements in the cellular responses around the implanted electrode including variable cell response over time and persistence of inflammation and scar formation at chronic time points. At 24 weeks of implantation, microgel-coated electrodes exhibited reduced astrocytic and activated

macrophage staining in the vicinity of the electrode. However, neuronal density close to the electrode was reduced for microgel-coated electrodes.

Cell adhesion studies were performed to compare mixed glial attachment between the uncoated and microgel-coated electrode surfaces. The mixed glial cells were chosen due to the presence of astrocytes and microglia, two of the main cell types involved in inflammation and scar formation. Microglial attachment studies have been performed by others[31] to observe differences in cell attachment to electrode surfaces. Monolayer microgel coatings have shown reduced protein adsorption[30,32] and reduced cell adhesion in other applications[19–21]. Quantification of *in vitro* data of multilayer coatings cultured with mixed glial cells showed promising results with significantly reduced cell adhesion on the electrode surface when coated with microgel particles. The significant reduction in cell spread area suggested the potential of the microgel coating for reducing cell adhesion in the early stages of cell-electrode interaction.

The *in vivo* data gathered from histological samples indicated a time-dependent tissue response surrounding neural electrodes. Staining for GFAP (astrocytes) around implanted electrodes at 1 week indicated the intensity$_1$, decay$_1$, and intensity$_2$ parameters were higher for microgel-coated samples, indicating increased astrocyte presence around the microgel-coated samples initially after implantation. From 1 week to 4 weeks the astrocyte staining parameters for uncoated samples increased for intensity$_1$ and decay$_1$ while decreasing for decay$_2$ while the microgel-coated sample parameters increased for intensity$_1$ and decay$_1$. This increase is a well-known response to chronically implanted electrodes and has been observed in multiple studies[9,24,28] as it is indicative of the scar formation that occurs over time around implanted electrodes. The 4 week time point showed increased staining for intensity$_1$, decay$_1$, and decay$_2$ parameters on microgel-coated samples while intensity$_2$ was higher for uncoated samples. These data indicate that astrocyte staining corresponding to the area closest to the electrode, was higher in the microgel-coated sample while the higher intensity$_2$ value for uncoated samples indicated increased astrocyte staining farther from the electrode at distances >100 μm. From 4 to 24 weeks microgel-coated sample parameters intensity$_1$ and decay$_1$ parameters decreased. All parameters for uncoated samples were higher than microgel-coated samples at 24 weeks. The change in parameters over time as well as at the 24 week time point indicated a reduction in astrocyte presence in response to the microgel-coated electrode, showing an improvement in one of the major constituents of the scar formation that occurs *in vivo*. Overall, the data indicate that GFAP staining increases initially and is maintained chronically as the intensity values indicate persistence of higher GFAP staining around the implanted electrode. These results are consistent with other studies reporting increasing astrocyte recruitment over time[9,18,28] as well as variation at different time points[24,25] indicating the variable nature of tissue response to implanted electrodes.

Staining for resident microglia using OX42/CD11b showed variability over time in tissue response to chronically implanted electrodes. At the 1 week time point, uncoated samples had higher intensity$_1$ and decay$_2$ parameters while decay$_1$ and intensity$_2$ were higher for microgel-coated samples. The data indicated higher resident microglial staining around uncoated electrodes in first phase of the decay equation corresponding to the 0–100 μm

distance from the electrode surface as well as faster decay of staining intensity in the second phase of the decay equation corresponding to the 100–500 μm distance from the implantation site. Conversely, higher microglial staining at the 100–500 μm distance indicates increased microglial presence away from the electrode site as well as faster decay of microglial staining intensity closest to the electrode surface around microgel-coated samples. The $decay_1$ parameter for microgel-coated samples increased from 1 to 4 weeks, indicating a faster decay in resident microglial presence at short time points close to the electrode surface. For the same time frame, uncoated sample $decay_2$ decreased indicating a slower decline in the resident microglial staining at distances 100–500 μm from the electrode surface. By 4 weeks all parameters for microgel-coated samples were higher than uncoated samples indicating increased microglial presence around microgel-coated samples. From 4 to 24 weeks $decay_1$ decreased for microgel-coated samples, and at 24 weeks uncoated electrode parameters were higher than microgel-coated electrode parameters for $intensity_1$ and $decay_1$ and lower for $intensity_2$. The changes at later time points indicate higher microglial staining around uncoated samples at distances close to the electrode surface while microgel-coated samples had higher staining at distances farther from the electrode surface at 100–500 μm from the implant. Overall, the variations in tissue response over time are similar to results observed in other studies of microglial response with an initial increase after implantation followed by fluctuations over time[25] as the tissue is constantly changing around the implant.

Response of activated microglia to the implanted electrodes also showed temporal changes in the reactivity of astrocytes in surrounding tissue. Activated microglia (ED1/CD68) staining parameters showed higher $intensity_1$ and $intensity_2$ for uncoated samples at 1 week, indicating higher microglial activation after initial implantation. From 1 to 4 weeks, the microgel-coated $decay_1$ parameter increased while uncoated $decay_1$ and $intensity_2$ decreased, resulting in higher $intensity_1$, $intensity_2$, and $decay_2$ and lower $decay_1$ for uncoated samples compared to microgel-coated samples at 4 weeks. These data indicate the increased presence of activated microglia around uncoated electrodes with parameters associated with both phases of the decay equation, which corresponds to distance both close to (0–100 μm) and farther (100–500 μm) from the electrode surface and is consistent with previously reported results[28]. The lower $decay_1$ parameter also indicates a slower decay around uncoated samples in the area closest to the electrode. From 4 to 24 weeks, parameters for uncoated electrodes increased for $intensity_1$ and $decay_1$, while $decay_1$ decreased for microgel-coated samples. At 24 weeks $intensity_1$, $decay_1$, and $intensity_2$ were higher and $decay_2$ was lower for uncoated samples. These data indicate maintenance of microglial activation around uncoated samples across the 500 μm analysis area, but also indicate a faster decay rate in staining close to the implanted electrode and slower decay rate farther from the electrode surface. The variation in ED1 activity over time is consistent with observations in the literature[25] as long-term studies have observed a similar response. As with the GFAP and OX42 markers, each cell response is variable over time with parameters that change between time points.

NeuN stain was used to identify neuronal nuclei in the area around implanted electrodes. At 1 week there were significant differences between the uncoated and contralateral (uninjured control) NeuN+ counts, as well as between the microgel-coated and contralateral samples at

0–100 μm and 100–200 μm for both groups. This indicates a decrease in neuronal density close to the electrode surface soon after implantation, and this trend is similar to what has been observed in literature.[24,28] At 4 weeks, the neuronal density around uncoated samples was significantly lower than microgel-coated samples at 0–100μm, and both groups were significantly lower than the contralateral control at the same distance. Additionally, the uncoated samples were significantly lower than the contralateral control at 200–300 μm. These data indicate the continued effect of the electrode presence in reducing neuronal cell density near the electrode surface, as constant presence of the electrode in the tissue continues to affect neuronal survival[28]. At 24 weeks, the microgel-coated samples had significantly lower neuronal density than the contralateral control at 0–100 μm and 100–200 μm, as well as significantly lower neuronal density compared to the 4 week time point in the 400–500 μm bin. This result was unexpected as we had hypothesized that the microgel-coating would improve the long-term cell response. We do not know the exact cause for the lower neuronal density around microgel-coated samples at 24 weeks. Overall, the data show lower neuronal staining levels near the implant, which increase as you move away from the injury. This behavior indicates the effect of the environment around the injury, likely a combination of physical injury from implantation as well as the resulting inflammatory response and cytokine release, which causes neuronal loss near the implant site. This is a significant problem for neural electrode function as neurons must be present near the site of the electrode for the implant to be functional in receiving neuronal signals.

Future work with microgel coatings can improve upon the material to make it more suitable for chronic neural electrode implantation. Several polymer coatings have been developed that demonstrate reduced protein adsorption and astrocytic recruitment around the implant[33,34], and others with reduced impedance and other improvements in conductive polymers to improve neuronal signal propagation.[35,36] One the of major responses that occurs after implantation of any material is the formation of scar-like tissue around the implant as the body tries to separate the implant from the tissue. The astrocytes and microglia in the brain contribute to this scar formation and it is believed that increased inflammation contributes to the activation of these cell types. Further modification of the microgel coatings with immunomodulators to control inflammation may contribute to greater improvements for tissue response to implanted electrodes. Release of anti-inflammatory agents can help to mediate the tissue response to a greater extent if the inflammation is controlled effectively. Many groups have attempted to modulate this inflammatory response with both passive and active release of anti-inflammatory factors. Zhong et al. developed a polymer coating with passive release of dexamethasone that showed a reduction in GFAP staining intensity, ED1 staining, and neuronal loss at 1 week and 4 weeks post-implantation[18]. Mercanzini et al. also demonstrated effectiveness of dexamethasone in a short term study to reduce astrocyte and microglial recruitment at 3 weeks[17]. Taub et al. showed the effectiveness of coatings containing IL-1ra compared to laminin coatings, demonstrating reductions in GFAP staining with the IL-1ra coating[37]. Others have tried to increase neuronal survival and attachment *in vitro*[11,13] however these coatings also improve cell attachment for unwanted cell types such as astrocytes. Additionally, the studies showing improvement in multiple cell types (astrocytes, microglia, and neurons) were only performed for short time points ~4 weeks. A recent study has

investigated long-term effects of Parylene-C coating for reducing cell adhesion on implanted silicon electrodes[14]. Although the results demonstrated reduced cell adhesion on the Parylene-C coated electrode, the inflammatory response persisted through the 12-week time point. We hypothesized that the composition of our microgel coating, containing temperature responsive pNIPAm combined with the “gold-standard” poly(ethylene glycol) for reducing cell adhesion, would provide a suitable alternative for reducing cell adhesion. Although both the Parylene-C coating presented by Winslow et al and the microgel coating presented in this study had reduced cell adhesion *in vitro*, the long-term *in vivo* observations indicated maintenance of long-term inflammatory response. Together, these studies indicate that the problem with chronically implanted electrodes goes beyond the need for a non-adhesive surface alone, but likely requires additional modification including inflammation attenuation. While many of these coatings showed some improvement there is no coating that solves all long-term tissue response problems, underscoring the need for further research. Our study indicated some improvement on certain parameters of GFAP, OX42, and ED1 staining with the microgel coating, similar to many of the studies listed above. However, maintaining long-term improvement for chronic time points is a difficult task which requires more investigation.

There are many areas for improvement in the area of neural electrode implantation. The response of the tissue surrounding the electrode is variable depending on the implant and the time point and continues to change over time. This variable environment provides a significant challenge for improving long-term electrode function, but we believe further modification of the electrode surface can provide options. Several labs have investigated the effects of modified electrode design geometry on the tissue response surrounding the electrode. Some groups have shown that while minimizing damage using smaller electrodes may provide some positive effects[38], the persistence of the electrode in the tissue remains a significant problem[7]. Modification of electrode design geometry[39,40] and insertion techniques[41] to minimize tissue injury and blood-brain-barrier disruption[42] may also provide better options. Another area of for potential improvement is the choice of electrode materials to improve upon the mechanical mismatch[43] that exists between stiff electrodes and soft neural tissue. Several groups have shown potential for improvement in tissue response when using materials that adapt after implantation with a resulting electrode that is softer and more mechanically similar to the brain tissue than stiff electrodes using computational[44] and experimentally validated models[45,46]. Using electrodes that are untethered has also indicated positive results compared to electrodes that are attached to the skull[38]. Adding neuron-specific survival and attractant factors[12] may also improve upon the recording potential, but these factors must also avoid recruitment of other cell types such as astrocytes which contribute to problematic scar formation.

The findings from many of these studies reiterate the importance of addressing the inflammatory response as inflammation is a factor that persists as part of the host response to implanted electrodes[47]. Long-term inflammation and microglial activation contribute to the foreign body response and failure of electrodes implanted for chronic time points[39]. Reduction of the inflammatory response can be achieved by releasing anti-inflammatory agents at the most beneficial time point, where specific drugs are targeted to be released at a time when the corresponding target molecule is at its peak in the inflammatory cascade. The

multi-faceted problem of improving long-term electrode functionality is a complicated task that will likely involve a combination of targets including reducing unwanted cell adhesion from astrocytes and microglia, maintaining neuronal survival and presence around the electrode, and reducing inflammation in the surrounding tissue. Modification of microgel-coated electrodes with anti-inflammatory agents to modulate inflammation around electrodes may provide an effective method for maintaining functionality of chronically implanted neural electrodes.

Supplementary Material

Refer to Web version on PubMed Central for supplementary material.

Acknowledgments

This work was supported by National Institutes of Health Grants: F31NS073358 (SMG) and T32EB006343-01A2 (RVB); GAANN Fellowship for Drug Design, Development, and Delivery: US Department of Education P200A090099; Georgia Tech/Emory Center for the Engineering of Living Tissues and the Atlanta Clinical and Translational Science Institute under PHS Grant UL RR025008 from the Clinical and Translational Science Award Program. XPS analysis was performed by the National ESCA and Surface Analysis Center for Biomedical Problems (NESAC/BIO): NIH EB-002027. We also thank Emily Herman from the Lyon lab for help with AFM imaging.

References

1. Schwartz AB, Cui XT, Weber DJ, Moran DW. Brain-controlled interfaces: movement restoration with neural prosthetics. Neuron. 2006; 52(1):205–20. [PubMed: 17015237]
2. Donoghue JP. Connecting cortex to machines: recent advances in brain interfaces. Nat Neurosci. 2002; 5(Suppl):1085–8. [PubMed: 12403992]
3. Lebedev MA, Nicolelis MA. Brain-machine interfaces: past, present and future. Trends Neurosci. 2006; 29(9):536–46. [PubMed: 16859758]
4. Birbaumer N, Cohen LG. Brain-computer interfaces: communication and restoration of movement in paralysis. J Physiol. 2007; 579(Pt 3):621–36. [PubMed: 17234696]
5. Anderson JM, Rodriguez A, Chang DT. Foreign body reaction to biomaterials. Semin Immunol. 2008; 20(2):86–100. [PubMed: 18162407]
6. Shain W, Spataro L, Dilgen J, Haverstick K, Retterer S, Isaacson M, Saltzman M, Turner JN. Controlling cellular reactive responses around neural prosthetic devices using peripheral and local intervention strategies. Ieee Transactions on Neural Systems and Rehabilitation Engineering. 2003; 11(2):186–188. [PubMed: 12899270]
7. Szarowski DH, Andersen MD, Retterer S, Spence AJ, Isaacson M, Craighead HG, Turner JN, Shain W. Brain responses to micro-machined silicon devices. Brain Res. 2003; 983(1–2):23–35. [PubMed: 12914963]
8. Turner JN, Shain W, Szarowski DH, Andersen M, Martins S, Isaacson M, Craighead H. Cerebral astrocyte response to micromachined silicon implants. Exp Neurol. 1999; 156(1):33–49. [PubMed: 10192775]
9. Polikov VS, Tresco PA, Reichert WM. Response of brain tissue to chronically implanted neural electrodes. J Neurosci Methods. 2005; 148(1):1–18. [PubMed: 16198003]
10. Cui X, Lee VA, Raphael Y, Wiler JA, Hetke JF, Anderson DJ, Martin DC. Surface modification of neural recording electrodes with conducting polymer/biomolecule blends. J Biomed Mater Res. 2001; 56(2):261–72. [PubMed: 11340598]
11. Azemi E, Gobbel GT, Cui XT. Seeding neural progenitor cells on silicon-based neural probes. J Neurosurg. 2010; 113(3):673–81. [PubMed: 20151783]
12. Cui X, Wiler J, Dzaman M, Altschuler RA, Martin DC. In vivo studies of polypyrrole/peptide coated neural probes. Biomaterials. 2003; 24(5):777–87. [PubMed: 12485796]

13. Jun SB, Hynd MR, Dowell-Mesfin NM, Al-Kofahi Y, Roysam B, Shain W, Kim SJ. Modulation of cultured neural networks using neurotrophin release from hydrogel-coated microelectrode arrays. J Neural Eng. 2008; 5(2):203–13. [PubMed: 18477815]
14. Winslow BD, Christensen MB, Yang WK, Solzbacher F, Tresco PA. A comparison of the tissue response to chronically implanted Parylene-C-coated and uncoated planar silicon microelectrode arrays in rat cortex. Biomaterials. 2010; 31(35):9163–72. [PubMed: 20561678]
15. Zhong Y, Bellamkonda RV. Controlled release of anti-inflammatory agent alpha-MSH from neural implants. J Control Release. 2005; 106(3):309–18. [PubMed: 15978692]
16. Kim DH, Martin DC. Sustained release of dexamethasone from hydrophilic matrices using PLGA nanoparticles for neural drug delivery. Biomaterials. 2006; 27(15):3031–7. [PubMed: 16443270]
17. Mercanzini A, Reddy ST, Velluto D, Colin P, Maillard A, Bensadoun JC, Hubbell JA, Renaud P. Controlled release nanoparticle-embedded coatings reduce the tissue reaction to neuroprostheses. J Control Release. 2010; 145(3):196–202. [PubMed: 20447428]
18. Zhong Y, Bellamkonda RV. Dexamethasone-coated neural probes elicit attenuated inflammatory response and neuronal loss compared to uncoated neural probes. Brain Res. 2007; 1148:15–27. [PubMed: 17376408]
19. Singh N, Bridges AW, Garcia AJ, Lyon LA. Covalent tethering of functional microgel films onto poly(ethylene terephthalate) surfaces. Biomacromolecules. 2007; 8(10):3271–5. [PubMed: 17877399]
20. Bridges AW, Singh N, Burns KL, Babensee JE, Andrew Lyon L, Garcia AJ. Reduced acute inflammatory responses to microgel conformal coatings. Biomaterials. 2008; 29(35):4605–15. [PubMed: 18804859]
21. Bridges AW, Whitmire RE, Singh N, Templeman KL, Babensee JE, Lyon LA, Garcia AJ. Chronic inflammatory responses to microgel-based implant coatings. J Biomed Mater Res A. 2010; 94A(1):252–258. [PubMed: 20166218]
22. Kipke DR, Vetter RJ, Williams JC, Hetke JF. Silicon-substrate intracortical microelectrode arrays for long-term recording of neuronal spike activity in cerebral cortex. IEEE Trans Neural Syst Rehabil Eng. 2003; 11(2):151–5. [PubMed: 12899260]
23. Hermanson, GT. Bioconjugate techniques. San Diego, CA: Academic Press; 1996.
24. McConnell GC, Rees HD, Levey AI, Gutekunst CA, Gross RE, Bellamkonda RV. Implanted neural electrodes cause chronic, local inflammation that is correlated with local neurodegeneration. J Neural Eng. 2009; 6(5):056003. [PubMed: 19700815]
25. Potter KA, Buck AC, Self WK, Capadona JR. Stab injury and device implantation within the brain results in inversely multiphasic neuroinflammatory and neurodegenerative responses. J Neural Eng. 2012; 9(4):046020. [PubMed: 22832283]
26. McConnell GC, Butera RJ, Bellamkonda RV. Bioimpedance modeling to monitor astrocytic response to chronically implanted electrodes. J Neural Eng. 2009; 6(5):055005. [PubMed: 19721187]
27. Kim YT, Hitchcock RW, Bridge MJ, Tresco PA. Chronic response of adult rat brain tissue to implants anchored to the skull. Biomaterials. 2004; 25(12):2229–37. [PubMed: 14741588]
28. Biran R, Martin DC, Tresco PA. Neuronal cell loss accompanies the brain tissue response to chronically implanted silicon microelectrode arrays. Exp Neurol. 2005; 195(1):115–26. [PubMed: 16045910]
29. South AB, Whitmire RE, Garcia AJ, Lyon LA. Centrifugal deposition of microgels for the rapid assembly of nonfouling thin films. ACS Appl Mater Interfaces. 2009; 1(12):2747–54. [PubMed: 20356152]
30. Nolan CM, Reyes CD, Debord JD, Garcia AJ, Lyon LA. Phase transition behavior, protein adsorption, and cell adhesion resistance of poly(ethylene glycol) cross-linked microgel particles. Biomacromolecules. 2005; 6(4):2032–9. [PubMed: 16004442]
31. Leung BK, Biran R, Underwood CJ, Tresco PA. Characterization of microglial attachment and cytokine release on biomaterials of differing surface chemistry. Biomaterials. 2008; 29(23):3289–97. [PubMed: 18485471]
32. Gan DJ, Lyon LA. Synthesis and protein adsorption resistance of PEG-modified poly(Nisopropylacrylamide) core/shell microgels. Macromolecules. 2002; 35(26):9634–9639.

33. Klaver CL, Caplan MR. Bioactive surface for neural electrodes: decreasing astrocyte proliferation via transforming growth factor-beta1. J Biomed Mater Res A. 2007; 81(4):1011–6. [PubMed: 17265435]
34. Lu Y, Wang D, Li T, Zhao X, Cao Y, Yang H, Duan YY. Poly(vinyl alcohol)/poly(acrylic acid) hydrogel coatings for improving electrode-neural tissue interface. Biomaterials. 2009; 30(25): 4143–51. [PubMed: 19467702]
35. Widge AS, Jeffries-El M, Cui X, Lagenaur CF, Matsuoka Y. Self-assembled monolayers of polythiophene conductive polymers improve biocompatibility and electrical impedance of neural electrodes. Biosens Bioelectron. 2007; 22(8):1723–32. [PubMed: 17015008]
36. Richardson-Burns SM, Hendricks JL, Martin DC. Electrochemical polymerization of conducting polymers in living neural tissue. J Neural Eng. 2007; 4(2):L6–L13. [PubMed: 17409471]
37. Taub AH, Hogri R, Magal A, Mintz M, Shacham-Diamand Y. Bioactive anti-inflammatory coating for chronic neural electrodes. J Biomed Mater Res A. 2012; 100(7):1854–8. [PubMed: 22488754]
38. Thelin J, Jorntell H, Psouni E, Garwicz M, Schouenborg J, Danielsen N, Linsmeier CE. Implant size and fixation mode strongly influence tissue reactions in the CNS. PLoS One. 2011; 6(1):e16267. [PubMed: 21298109]
39. Skousen JL, Merriam SM, Srivannavit O, Perlin G, Wise KD, Tresco PA. Reducing surface area while maintaining implant penetrating profile lowers the brain foreign body response to chronically implanted planar silicon microelectrode arrays. Prog Brain Res. 2011; 194:167–80. [PubMed: 21867802]
40. Seymour JP, Kipke DR. Neural probe design for reduced tissue encapsulation in CNS. Biomaterials. 2007; 28(25):3594–607. [PubMed: 17517431]
41. Nicolelis MA, Dimitrov D, Carmena JM, Crist R, Lehew G, Kralik JD, Wise SP. Chronic, multisite, multielectrode recordings in macaque monkeys. Proc Natl Acad Sci U S A. 2003; 100(19):11041–6. [PubMed: 12960378]
42. Bjornsson CS, Oh SJ, Al-Kofahi YA, Lim YJ, Smith KL, Turner JN, De S, Roysam B, Shain W, Kim SJ. Effects of insertion conditions on tissue strain and vascular damage during neuroprosthetic device insertion. J Neural Eng. 2006; 3(3):196–207. [PubMed: 16921203]
43. Lacour SP, Benmerah S, Tarte E, FitzGerald J, Serra J, McMahon S, Fawcett J, Graudejus O, Yu Z, Morrison B 3rd. Flexible and stretchable micro-electrodes for in vitro and in vivo neural interfaces. Med Biol Eng Comput. 2010; 48(10):945–54. [PubMed: 20535574]
44. Subbaroyan J, Martin DC, Kipke DR. A finite-element model of the mechanical effects of implantable microelectrodes in the cerebral cortex. J Neural Eng. 2005; 2(4):103–13. [PubMed: 16317234]
45. Capadona JR, Tyler DJ, Zorman CA, Rowan SJ, Weder C. Mechanically adaptive nanocomposites for neural interfacing. Mrs Bulletin. 2012; 37(6):581–589.
46. Harris JP, Hess AE, Rowan SJ, Weder C, Zorman CA, Tyler DJ, Capadona JR. In vivo deployment of mechanically adaptive nanocomposites for intracortical microelectrodes. J Neural Eng. 2011; 8(4):046010. [PubMed: 21654037]
47. Winslow BD, Tresco PA. Quantitative analysis of the tissue response to chronically implanted microwire electrodes in rat cortex. Biomaterials. 2010; 31(7):1558–67. [PubMed: 19963267]

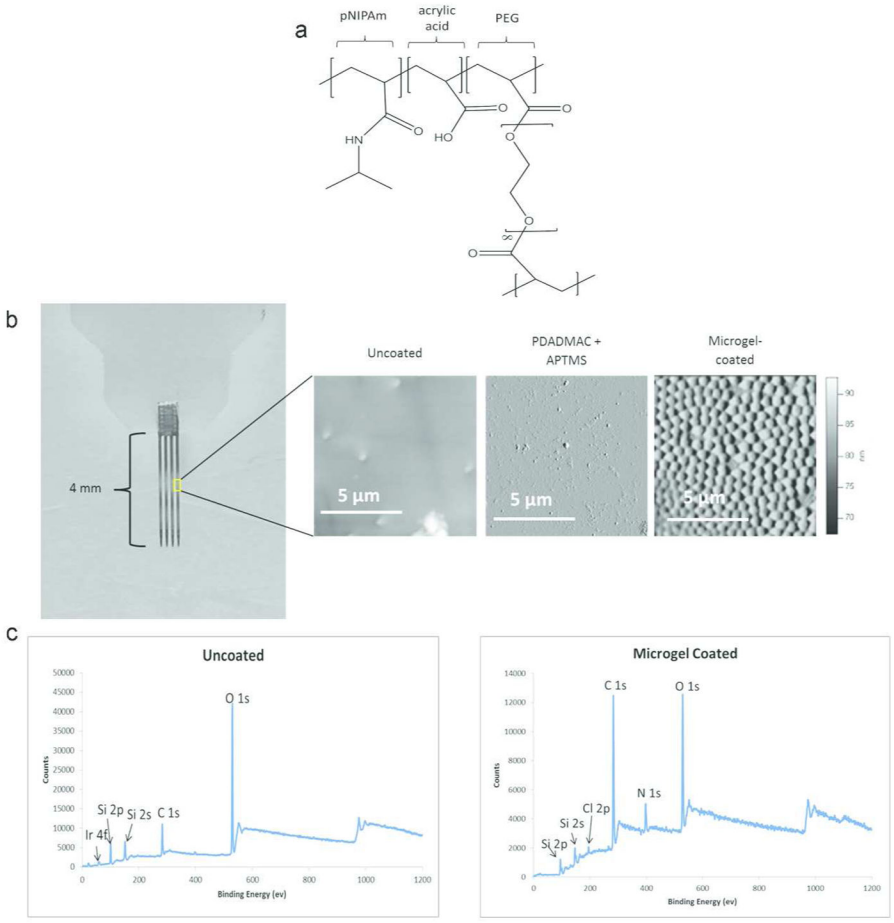

Figure 1.

Microgel coatings applied to the surface of the neural electrode. (a) Chemical structure of the microgel contains pNIPAm, PEG, and acrylic acid. (b) Photo of the neural electrode (left) with AFM scans for uncoated, PDADMAC+APTMS only, and multi-layer microgel-coated surfaces. The microgel coating application was further verified using X-ray electron spectroscopy to verify differences between the uncoated and microgel-coated (c) surfaces with the absence of iridium 4f peak and prominent C1s and N1s peaks on the microgel-coated sample.

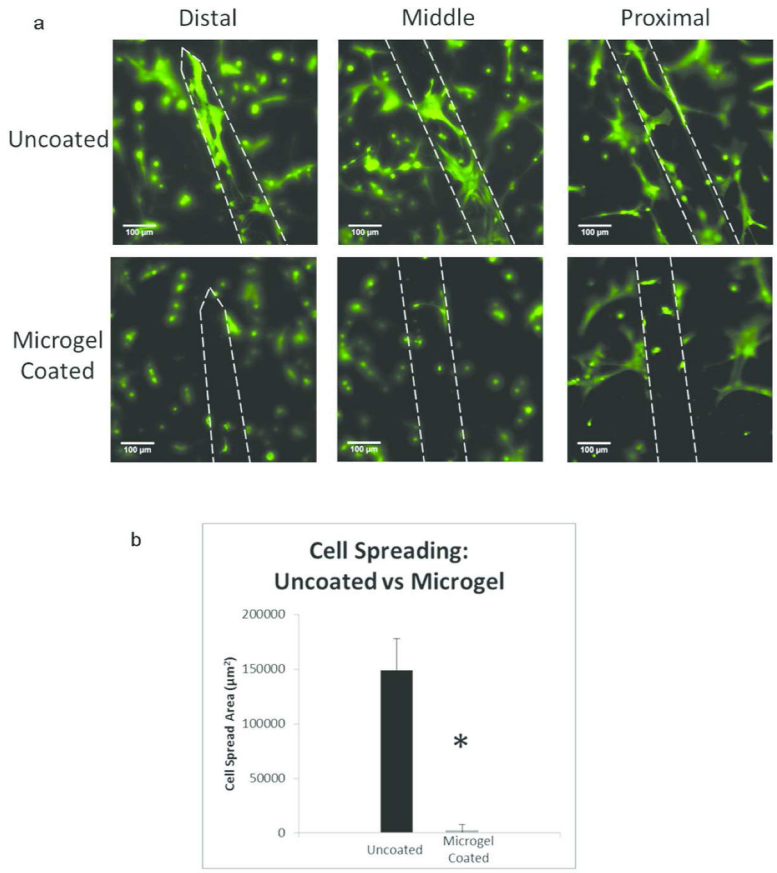

Figure 2.

Microgel coatings reduce *in vitro* mixed glial cell adhesion on electrodes. Electrodes were plated with mixed glial cells (astrocytes and microglia) and cultured for 24 hours. Samples were stained using LIVE/DEAD stain (Invitrogen) and imaged using fluorescence microscopy (a). Cell spreading area was analyzed using ImageJ to determine the amount of cell spread area for each group (b). Microgel coatings reduced cell adhesion on the electrode surface compared to uncoated controls ($p<0.01$). Data is presented as mean ± standard error of the mean, n=3 electrodes. Scale bars = 100µm.

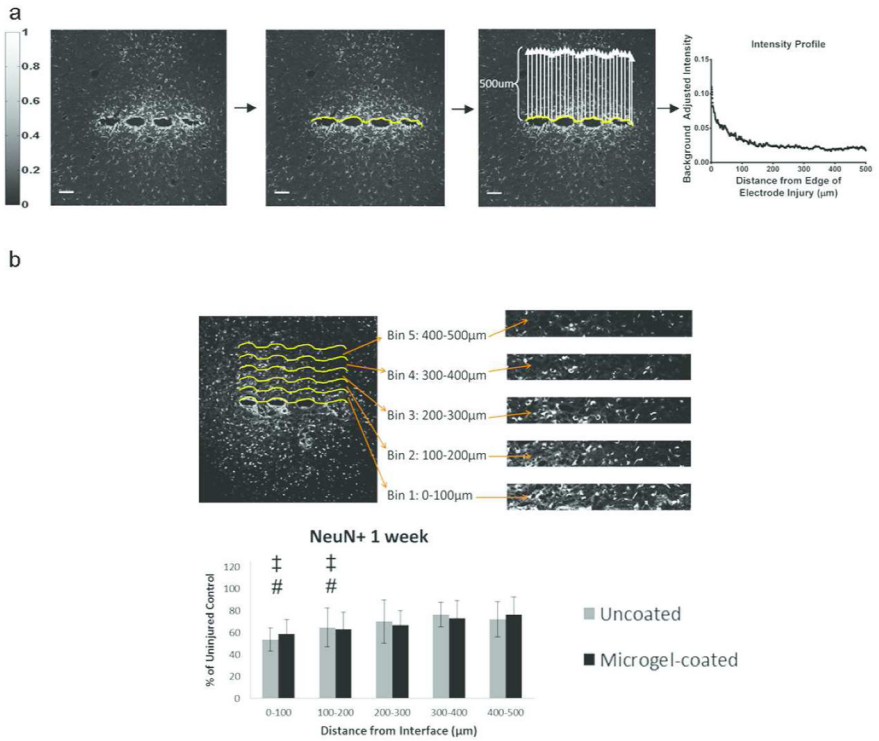

Figure 3.

Analysis of immunostaining was performed using a custom MATLAB program. (a) The IHC images for each sample of GFAP, OX42, or ED1 stained sections were displayed and a curve generated along the edge of the scar formed by the electrode. A scale bar (left) indicates the intensity values of the staining from 0 (black) to 1 (white). The program determines the average of the intensity along the curve from 0–500μm away from the scar and generates an intensity curve as a function of distance. Sample intensity curve is shown from an uncoated electrode at 24 weeks for GFAP stain (a, right). This curve is fit with Equation 1 and parameters for each curve are compared between groups. Image processing for NeuN stained samples (b) involves dividing the 500 μm image into 5 equal-sized bins of 100 μm and counting NeuN positive cells in each bin. These NeuN+ cell counts are compared to the uninjured control from the contralateral hemisphere. Scale bar = 100 μm.

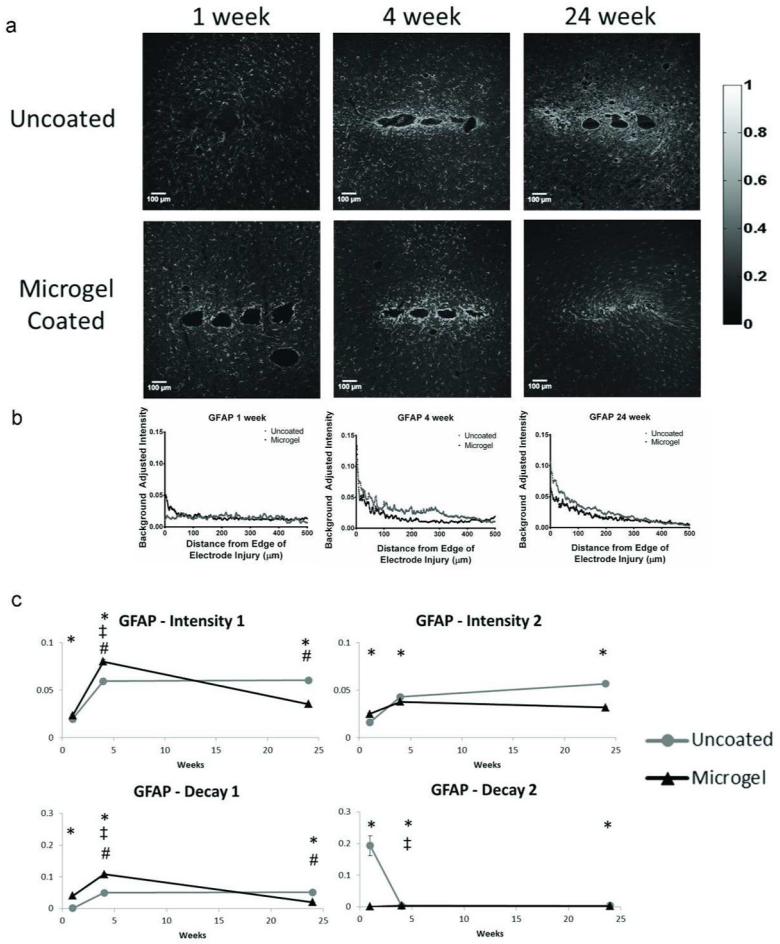

Figure 4.

Immunohistochemistry images and corresponding intensity scale (a) from each time point and group of samples stained with glial fibrillary acidic protein (GFAP), a marker for astrocytes (n=4 animals for all groups except n=3 for uncoated at 24 weeks). Curve fits on each intensity curve are completed using Equation 1. Representative intensity curves from background-corrected images (b) are located below the representative immunostaining images for each time point. Parameter curves (c) indicate changes in parameter values over time for the experimental groups. Symbols indicate: ***** significant differences between the groups at one time point, ‡ significant differences over time between the indicated and preceding time-point for uncoated samples, # significant differences over time between the indicated and preceding time-point for microgel-coated samples.

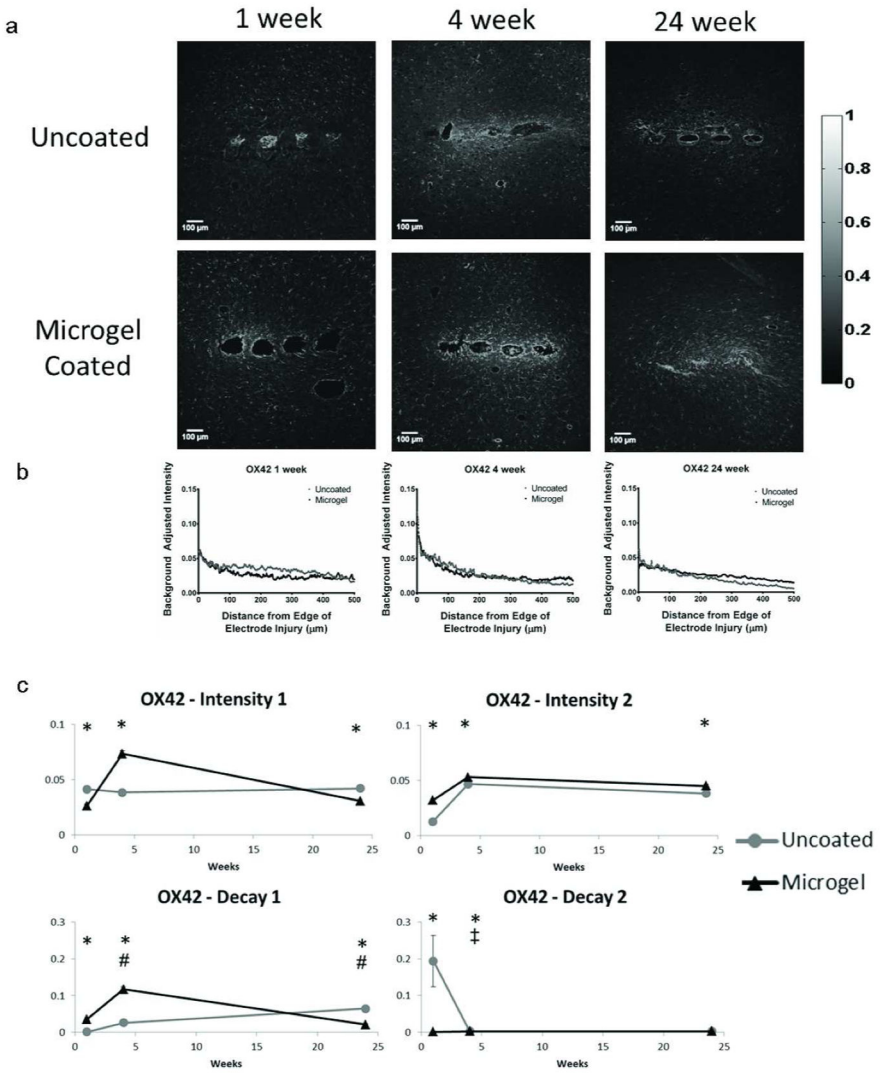

Figure 5.

Immunohistochemistry images and corresponding intensity scale (a) from each time point and group of samples stained with OX42 (CD11b), a marker for microglia. Representative intensity curves from background-corrected images (b) are located below the representative immunostaining images for each time point. Parameter curves (c) were generated in a similar manner to those for GFAP and indicate changes in intensity and decay values over time for the experimental groups. Symbols indicate: ***** significant differences between the groups at one time point, ‡ significant differences over time between the indicated and preceding time-point for uncoated samples, # significant differences over time between the indicated and preceding time-point for microgel-coated samples.

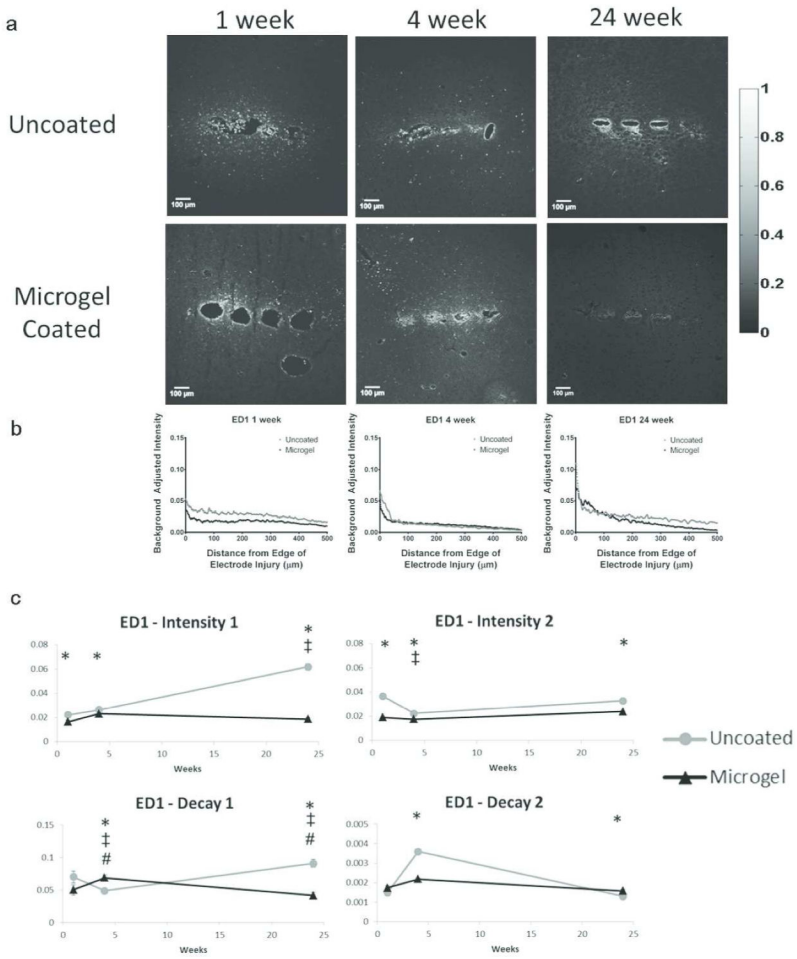

Figure 6.

Immunohistochemistry images and corresponding intensity scale (a) from each time point and group of samples stained with ED1 (CD68), a marker for activated microglia. Representative intensity curves from background-corrected images (b) are located below the representative immunostaining images for each time point. Parameter curves (c) were generated in a similar manner to those for GFAP and indicate changes in parameter values over time for the experimental groups. Symbols indicate: ***** significant differences between the groups at one time point, ‡ significant differences over time between the indicated and preceding time-point for uncoated samples, # significant differences over time between the indicated and preceding time-point for microgel-coated samples.

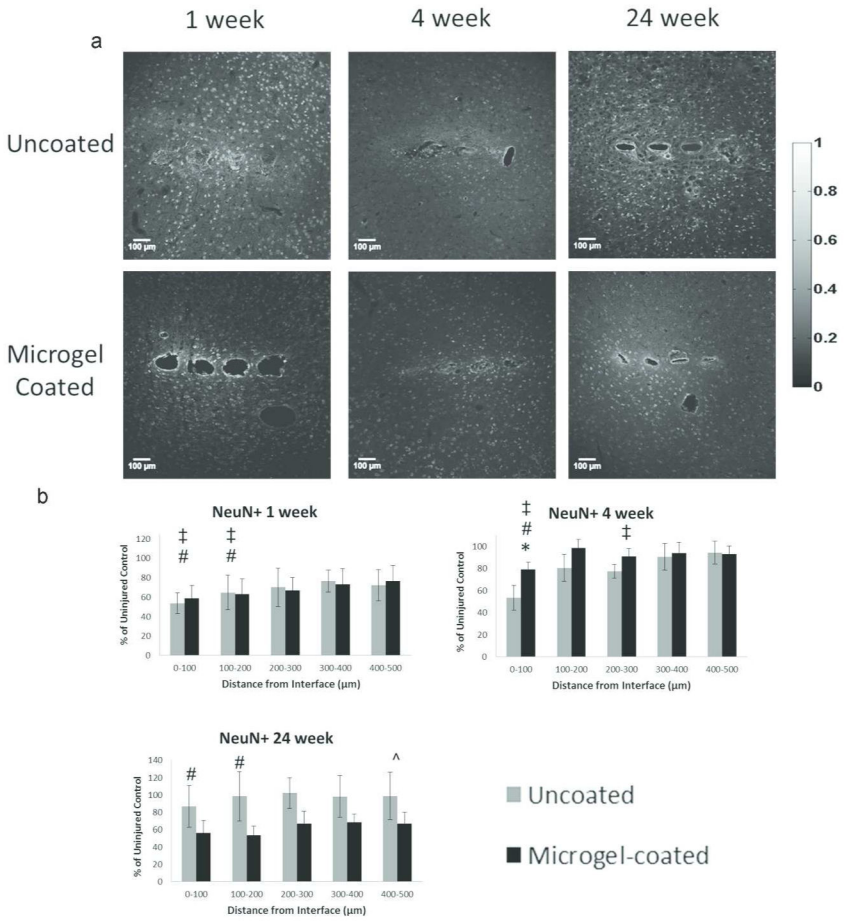

Figure 7.

Immunohistochemistry images (a) from each time point and experimental group stained with NeuN, a marker for neuronal. Graphs for each time point (b) indicate the average number of neuronal nuclei in each 100μm bin for uncoated and microgel-coated samples as a percentage of the cells found in the contralateral uninjured control. Symbols indicate: ***** significant differences between uncoated and microgel-coated samples, ‡ significant differences between uncoated and contralateral samples, # significant differences between microgel-coated and contralateral samples, ^ significant differences between the indicated and preceding time-point for microgel-coated samples.

Table 1

Antibodies utilized for immunofluorescence analysis

Antibody	Supplier	Cell Type
Glial fibrillary acidic protein (GFAP)	Abcam ab7260	Astrocytes
NeuN	Millipore MAB377	Neuronal nuclei
OX42/CD11b	Chemicon CBL1512	Resident microglia
ED1/CD68	AbD Serotec MCA341R	Activated microglia